A Multilayer Front-End for an Imaging Radar Sensor

Mario Leib[1], Winfried Mayer[1], Horst Bilzer[2] and Wolfgang Menzel[1]

[1] University of Ulm, Microwave Techniques, Albert-Einstein-Allee 41, 89081 Ulm, Germany
[2] now with: EADS Ewation GmbH, Wörthstr. 85, 89077 Ulm, Germany

***Abstract* — In this contribution a compact multilayer front-end for a 24 GHz FM-CW imaging radar sensor is presented. After a brief review of the sensor concept the front-end's design and realization are described. The front-end consists of one transmitter stage followed by a switched transmit array with 25 antenna elements and two non-switched coherent receivers. Key structures of the multilayer printed circuit board (PCB) design are the contacting areas of MMICs, space saving RF feed-throughs and the antenna. Solutions for these structures are presented in detail together with exemplary test results. Successful realization and tests demonstrate that a front-end module for an electronically scanning sensor can be realized in multilayer PCB technology at moderate cost.**

***Index Terms* — automotive sensors, FM-CW radar, interconnections, radar imaging, radar sensor**

I. Introduction

In the past years many radar sensors for automotive applications like adaptive cruise control (ACC), collision warning and parking aid have been developed [1]–[4]. Current research is on multi-functional sensors which can meet several features by two dimensional imaging (angle and range) of a large field of view in front of a car. Small size and low cost are additional requirements set up by the automotive application.

One approach to achieve these goals is to use a bistatic FM-CW radar with switched antennas [5], [6]. By processing data from successively performed range scans for different transmit or receive antennas, angular resolution and therefore two dimensional imaging is possible with moderate RF hardware effort. In [6] a first prototype of a sensor architecture with 25 switched transmit and two parallel receive elements is presented, and its operation principle is demonstrated by exemplary radar images. In this paper an improved compact RF front-end for the sensor in [6] is described in detail with the focus on realization and integration of the RF building blocks. All RF circuitry, supporting electronics and the antenna array are integrated in one multilayer substrate.

II. Front-End Architecture

The sensor principle is based on a switched antenna array and two separate receiving channels. This section gives a short description of the front-end architecture by means of the block diagram in Fig. 1. For the operation principle [6] can be referenced.

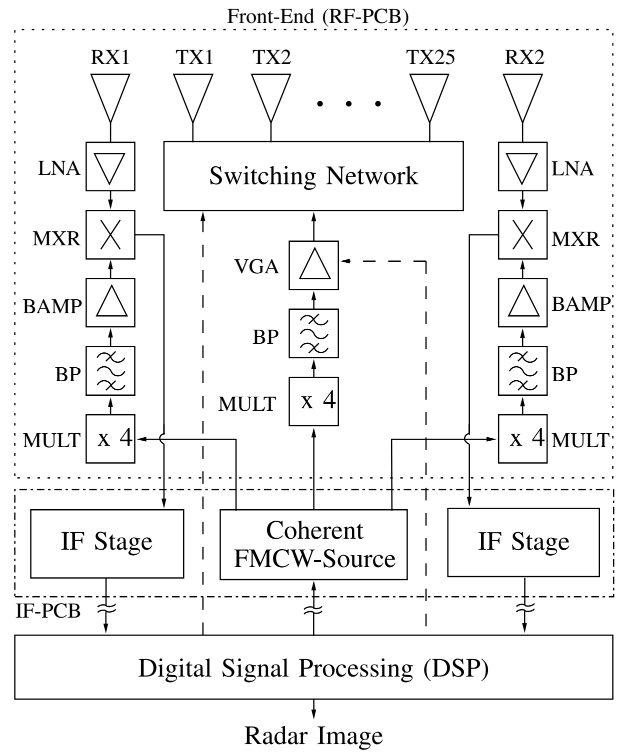

Fig. 1. Block diagram of the sensor front-end.

The transmit signal is generated by a FM-CW source using a phase locked loop (PLL) for frequency stabilization and a direct digital synthesizer (DDS) for waveform generation. The transmit switching network connects the 25 transmitting antennas (TX1-TX25) successively to the transmitting stage. To compensate the insertion losses of the switches a variable gain amplifier (VGA) is installed at the input of the switching network. All elements of the antenna array are positioned equally with half a wavelength distance at the operating frequency.

Signals reflected by obstacles ahead of the car are received in parallel by two antennas located left (RX1) and right (RX2) to the transmit stage. These receiving antennas have the same shape as the transmit antennas. All antenna

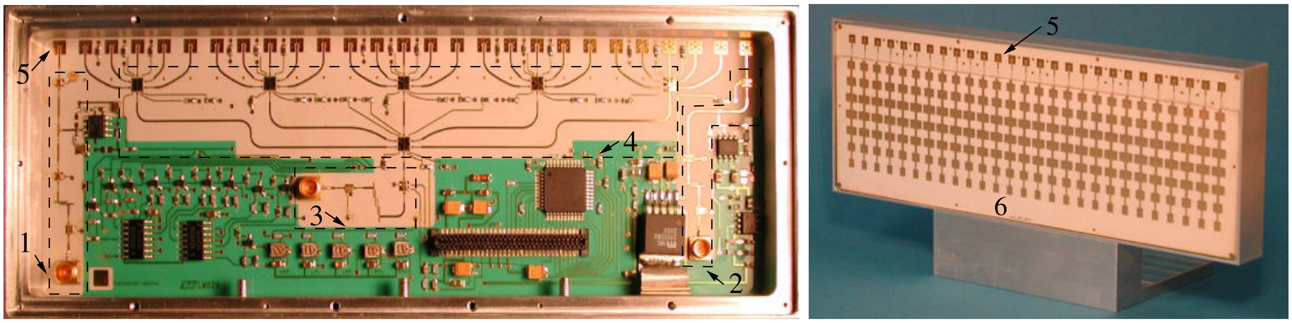

(a) Backside of the sensor front-end (component side).

(b) Front view (antenna side).

Fig. 2. Photographs of the realized front-end PCB including casing and mounting.

elements are linearly arranged and can be fabricated on a single substrate. Both receiving blocks are identical with a low noise amplifier (LNA) after the antenna, followed by a down-converter (MXR) and the local oscillator path. To adjust the local oscillator input power of the down-converter, a buffer amplifier (BAMP) is necessary. Within the intermediate frequency (IF) stage, amplification and analog processing of the base band signals is done. The IF stage is placed on a separate PCB (IF-PCB), together with the FM-CW source, operating at lower frequencies. Finally, the radar images are calculated from sampled and digitized data in a remote signal processing unit (DSP).

III. Front-End Design

In order to guide the RF signals using microstrips on both sides of the front-end (RF-PCB), two $0.2\,\mathrm{mm}$ thick low cost RF substrates are laminated on both sides of a $0.8\,\mathrm{mm}$ FR4 core with prepreg material. Inner FR4 layers are used to route the DC signals. In Fig. 2 the realized front-end is displayed in front and backside view. The dimensions are $175\,\mathrm{mm} \times 65\,\mathrm{mm} \times 16\,\mathrm{mm}$.

Both receivers (1, 2), the transmitting stage (3) and the switching network (4) are placed on the backside of the RF-PCB (component side). In addition, control logics for the switches, their driver stages, and the MMIC biasing circuitry are located on this PCB side. For the active RF components and the mixers, commercial MMICs are used. The bandpass filters to suppress harmonics are implemented as parallel-coupled $\lambda/2$-resonators. The switching network consists of six SP5T switch MMICs [7] and is arranged symmetrically. Phase differences from the different lengths of the transmit paths are taken into account in the digital signal processing. The necessary phase information can be obtained by a near field measurement. To transfer the $6\,\mathrm{GHz}$ source signal from the IF-PCB to the RF-PCB, commercial RF connectors are applied, permitting to stack both PCBs directly onto each other. In this way, a compact module with a depth of less than $18\,\mathrm{mm}$ can be achieved. As all MMICs are on the backside of the RF-PCB, they are protected and shielded by the stacked IF-PCB. To guide the RF signal from the component side of the RF-PCB to the antenna side, a special and easily manufacturable RF feed-through (5) is necessary. This RF feed-through as well as the antenna array (6) on the frontside are described in detail in section IV.

IV. Key Structures

A. Contacting area of MMICs

All MMICs are mounted on a ground metalization on the top side of the PCB. This area is connected to a continuous ground plane on the backside of the RF substrate by using vias. The MMIC signal pads are contacted to the microstrips by bond wires. Inductive and capacitive effects of the bond wires are compensated by a matching network consisting of two symmetrical line steps (see Fig. 3). In order to adapt the matching network to the given problem, the width and length of the smaller microstrip section (see (1) in Fig. 3) were optimized using the simulation software *Microwave Studio* [8].

To verify the effects of the matching network, the return loss of the used MMIC switch [7] with and without matching network has been measured. These measurement results are depicted in Fig. 3. With the matching network, the return loss improves significantly at $25\,\mathrm{GHz}$, so that a maximal insertion loss of $-2.2\,\mathrm{dB}$ instead of $-2.6\,\mathrm{dB}$ without matching network can be obtained. Therefore the matching network is used for each MMIC contacting area on the RF-PCB.

B. PCB feed-through

A main design challenge is to feed the RF signal from the backside to the frontside of the RF-PCB with a structure that can easily be fabricated in a standard PCB process. In Fig. 4 a cross section of the simulation model, and in the left corner of Fig. 5 a top view of the realized

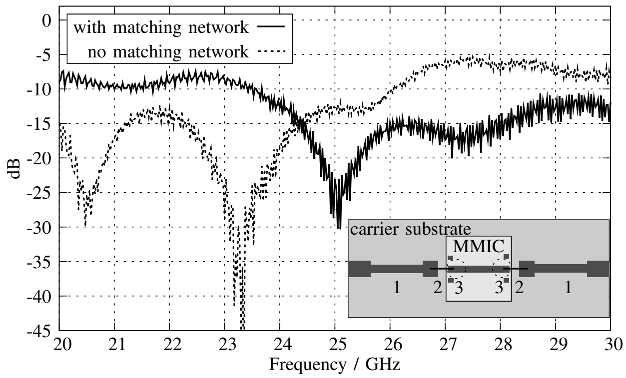

Fig. 3. Measured return loss of the MMIC connection with and without matching network. The inset in the diagram shows the top view of the case with the matching network (1: matching network, 2: bond wire, 3: carrier substrate ground via).

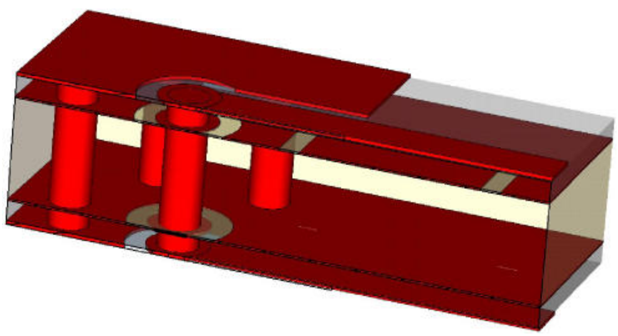

Fig. 4. Cross section view of the simulation model of the PCB feed-trough.

feed-through is displayed. The main task of the PCB feed-through is to transform the microstrip mode into a coaxial mode by using an appropriately shaped ground area on both sides of the PCB connected to each other with five ground vias. The RF via is placed in the center of the ground vias, connecting the microstrips on both sides to each other. Parallel plate modes in the inner layer, and so energy loss, are suppressed by two slots in the ground layers. This solution can be fabricated much easier than a structure with vias as these would have to be blind vias.

Fig. 5 shows the simulation [8] and measurement results of the PCB feed-through. As the transition is very sensitive to variances of the nominal value of the core thickness, production tolerances could cause the difference between simulation and measurement. Despite that difference the measured reflection coefficient is still better than -10 dB over a wide frequency range. The insertion loss is also quite good with less than -2 dB.

C. Antenna & Mounting

Each antenna element of the array is implemented as a linear series of seven patch antennas. The array is realized on a separate low cost RF substrate with a height of

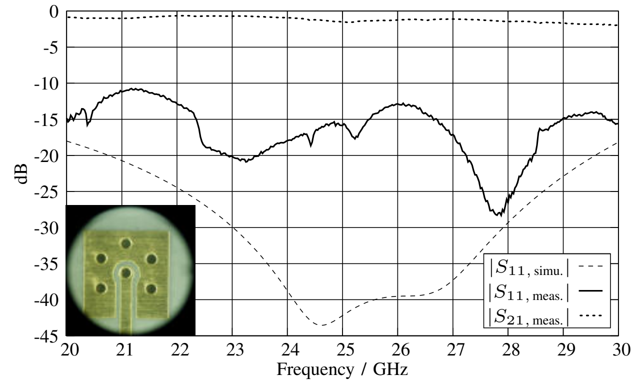

Fig. 5. Measured and simulated scattering parameters of the PCB feed-through (see microscope photograph).

0.5 mm for better radiation characteristics, resulting in a 3 dB-beamwidth of maximal $17°$ in elevation, a wide field of view in azimuth, and a gain of minimal 12 dBi from 24 GHz to 25 GHz. Sidelobes are suppressed by at least 9 dB in this frequency range, and the main beam changes slightly with frequency. Further optimization of the antenna elements will be done in the future.

The antenna substrate is mounted on the frontside (antenna side) of the RF-PCB using conductive glue. The microstrip lines on the antenna substrate and the top RF substrate (carrier substrate) are connected by a soldered silver wire with $150\,\mu$m diameter for a robust assembly. In addition, a via is necessary to connect the two ground planes (see inset in Fig. 6). To match the transition a common $\lambda/4$-transformer is used. The integration of an antenna structure in the frontside of the multilayer would require that many vias, necessary for DC routing, had to be buried. By using an separate antenna substrate on top of the multilayer all vias can be realized with through holes giving an overall benefit in production cost. This solution also gives flexibility to use different antenna substrates, e. g. one with an improved design.

Fig. 6 shows the measured scattering parameters and the cross section view of the transition. In the test structure used for measurement, the ground via has a diameter of 1.8 mm, and the distance between the ground via and the $\lambda/4$-transformer is $100\,\mu$m. As shown in the diagram, the matching is quite good, and a relative bandwidth of 20% at -15 dB has been achieved. Further simulations showed that the use of vias with a smaller diameter has almost no effect on the transmission behavior. Thus, only a via with a 0.4 mm diameter is used in the front-end realization for the antenna substrate transition.

V. Test Results

For the characterization of the transmitter of the realized front-end each radiation pattern of the 25 transmitting

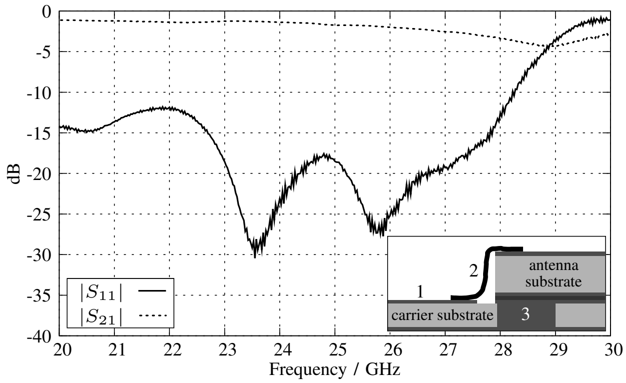

Fig. 6. Measured scattering parameters of the transition (see 2D cross section) between carrier substrate and antenna substrate (1: microstrip λ/4-transformer, 2: soldered wire, 3: ground via).

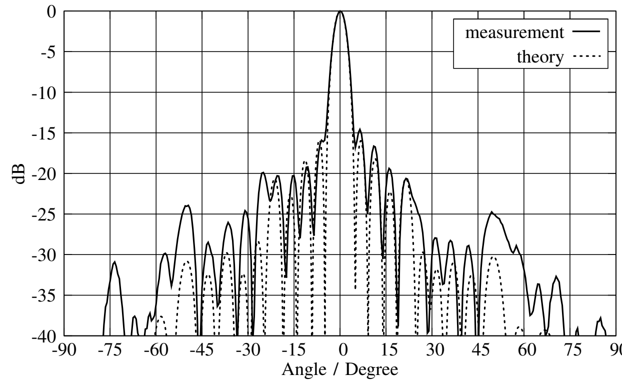

Fig. 7. Synthesized radiation diagram of the antenna array in azimuth at 24.5 GHz compared with theory.

antennas in H-plane was measured in amplitude and phase. Based on these data, the synthesized radiation pattern of the antenna array can be achieved by adding up the complex measurement values for all switch states at each measured angle. In addition, to obtain the radiation pattern in Fig. 7, the phase differences between the antennas due to the switching network have to be corrected. Phase angles and amplitudes of the antenna elements were measured using a near field measurement set-up. In principle, also the amplitude values can be weighted to improve the sidelobe performance. For the diagram in Fig. 7, however, only phase angles were corrected. The resulting radiation diagram has a 3 dB-beamwidth of $4.2°$ and a sidelobe suppression of 14.9 dB at 24.5 GHz. The theoretical result is obtained by multiplying the array factor (with amplitude taper) and the theoretical radiation pattern of a typical patch. The good agreement between measurement and theory of the synthesized radiation diagrams proves that the switched transmitter is qualified for the sensor principle.

The EIRP of a single array element vary between 10 dBm and 16 dBm in the frequency range of 24 GHz -25 GHz because of the switching network. For frequencies higher than 25 GHz performance degrades, but radar measurements are still possible up to 26 GHz. The gain of the two receivers from the LNA to the IF stage has a typically value of 30 dB from 24 GHz -25 GHz including an implemented IF preamplifier stage with a gain of about 20 dB. For frequencies higher than 25 GHz performance degrades, too. Therefore the front-end is suitable for a bandwidth of 1 GHz.

VI. Conclusion

A compact front-end realization for an automotive radar sensor with moderate cost has been presented. Some design aspects have been introduced and explained in detail. Measurement results for some of the structures and the antenna of the front-end have been shown, too.

The development of a DSP board for data acquisition is in progress, so that in the near future real time radar measurements can be made, and signal processing techniques can be tested. Furthermore, to reduce the cost of the front-end, GaAs switch MMICs can potentially be replaced by low cost switches on glass substrate [9] and the remaining GaAs MMICs by custom specific SiGe designs.

VII. Acknowledgment

These developments have been done partially within a cooperation between University of Ulm and Daimler-Chrysler AG, Research & Technology. Special thanks are due to Dr. Helmut Leier for his fruitful contributions and support.

References

[1] W. Mayer, M. Meilchen, W. Grabherr, P. Nüchter, and R. Gühl, "Eight-channel 77-GHz front-end module with high-performance synthesized signal generator for FM-CW sensor application," *IEEE Transactions on Microwave Theory and Techniques*, vol. 52, no. 3, pp. 29–38, March 2004.

[2] R. Mende and H. Rohling, "New automotive applications for smart radar systems," in *German Radar Symposium (GRS) Proceedings*, September 2002, pp. 35–40.

[3] M. Klotz and H. Rohling, "24 GHz radar sensors for automotive applications," in *International Conference on Microwaves, Radar and Wireless Communications (MIKON)*, May 2000, pp. 359–362.

[4] R. Schneider and J. Wenger, "System aspects for future automotive radar," in *IEEE Transactions on Microwave Theory and Techniques Symposium*, 1999, pp. 293–296.

[5] Y. Asano, S. Ohshima, T. Harada, M. Ogawa, and K. Nishikawa, "Proposal of millimeter-wave holographic radar with antenna switching," in *IEEE Transactions on Microwave Theory and Techniques Symposium*, vol. 2, 2001, pp. 1111–1114.

[6] W. Mayer, S. Buntz, H. Leier, and W. Menzel, "Imaging radar sensor front-end with a large transmit array," in *European Microwave Conference (EuMC)*, October 2004.

[7] Skyworks Solutions Inc., *23-26 GHz GaAs MMIC 6 Port Reflective PIN Switch*, December 2002.

[8] *Microwave Studio 5.0*, CST-Computer Simulation Technology.

[9] M/A-COM Inc., *SP4T monolithic PIN Diode Switch*.